Lift and Drag of a Wing-Cone Configuration in Hypersonic Flow

ADOLFO REGGIORI*
New York University, New York, N. Y.

Nomenclature

C_D = drag coefficient
C_L = lift coefficient
P = pressure
x = body axis
α = angle of attack
θ = defined in Fig. 2

Introduction

RECENTLY, a great interest has arisen in the study of hypersonic flight, in connection with high-speed transportation and re-entry vehicles. Requirements of maneuverability and long range flight impose the choice of vehicles with a relatively large lift-drag ratio. In order to gain information on the possible characteristics of such vehicles, a considerable effort is devoted to the study of bodies of simple shapes. A body which can give good lift and drag characteristics is a cone-wing configuration (Fig. 1); with this configuration an attempt is made to take advantage of the aerodynamic interference between the cone and the wing, which gives rise to a rather large increase in pressure on the windward side of the body, and a corresponding decrease on the leeward side. The present Note gives some results of a series of experiments performed to determine the pressure distribution and the total forces on a configuration consisting of a 20° cone with wings located at 60° from the plane of symmetry and sweepback angle of 75°. The Mach number of the experiments was equal to 5.8; in these conditions the leading edge of the wing was subsonic. The lift and drag coefficients have been determined from the pressure distribution and directly from balance measurements. The results are compared to those obtained with an isolated cone.

Test Apparatus

The experiments were performed in the Mach 6 wind tunnel at the New York University Aerospace Laboratory. The wind tunnel is of the blow-down type, with supply pressures ranging from 100 psia to 2000 psia and a stagnation temperature of 900°R. The test section is axis-symmetric with a diam of 12 in. The Mach number in the test section is equal to 5.8. The Reynolds number/ft ranges between 2×10^6 and 40×10^6, depending on the supply pressure. Two models were used for the experiments, both with the same configuration (Fig. 1); the first model had a base diam of 4.6 in. and was used for pressure measurements; the second

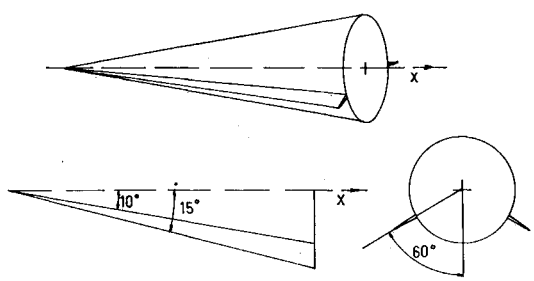

Fig. 1 Schematic wing-cone configuration.

Received October 17, 1970; revision received January 11, 1971.

* Assistant Research Scientist; now Research Scientist at Politecnico di Milano, Milano, Italy.

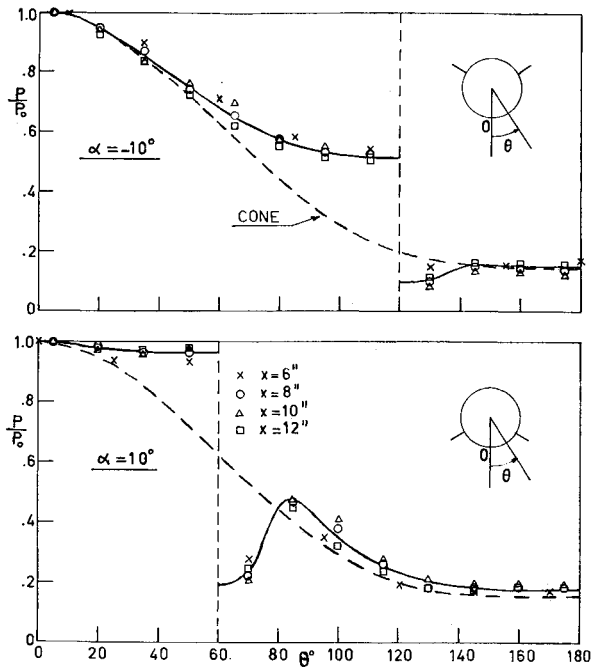

Fig. 2 Pressure distribution on the cone surface.

model had a base diam of 3.0 in. and was used for direct force measurements with a sting balance. All the data from the pressure taps and from the balance were recorded with a Honeywell Visicorder multichannel recorder. The recording of the pressure data required the use of three sampling valves; each valve was connected to a group of pressure taps in the model and to a different channel in the recorder. Each test had a duration of about 15 sec.

Results

Measurements of the pressure distribution were made on the first model at angles of attack equal to 0°, 5°, 10°, 15°, −5°, −10°. The experiments were performed at different supply pressures, ranging from 100 psia to 2000 psia. The pressure distribution was not affected by the variation of Reynolds number, except possibly on the leeward side near the wing, where the readings were rather scattered and could not be repeated even under identical test conditions. Two examples of the pressure distributions obtained on the surface of the cone are shown in Fig. 2. It appears very clearly that the interference effect of the wing is very strong at posi-

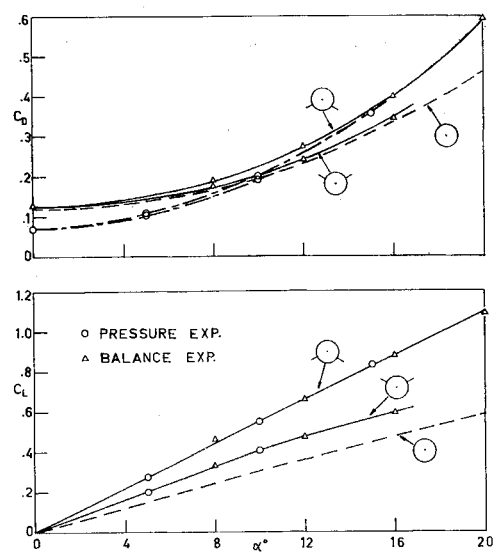

Fig. 3 Lift and drag coefficients vs angle of attack.

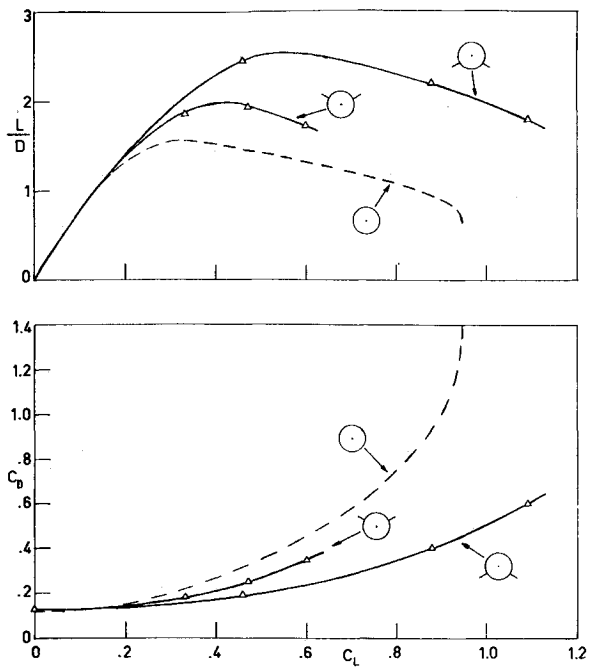

Fig. 4 Drag coefficient and life-drag ratio vs lift coefficient.

tive angle of attack (negative dihedral); the cross flow component on the windward side remains very small and the pressure results nearly constant in this region. On the leeward side the expansion on the back of the wing produces a region of low pressure on the cone; far from the wing (about 20° in this case) the interference practically disappears and the pressure distribution becomes similar to that obtained for an isolated cone. As a comparison, the pressure distribution computed with the Newtonian approximation for a 20° cone is also plotted. The larger pressure on the windward side acts to increase both the lift and the drag of the cone, whereas the expansion induced near the back of the wing acts practically only to reduce the drag (because in the region near $\theta = 90°$ the contribution of the pressure to the lift is very small). At negative angles of attack (positive dihedral) the interference effect of the wing appears to be less pronounced; this is explained by the fact that the wing is partially shaded by the cone surface. There is still a reduction in the cross flow and an increase of pressure on the windward side, especially near the wing, but this actually gives a negative contribution to the lift while the drag is increased.

The pressure on the wing was also measured; at angles of attack larger than 5° the pressure results practically constant on the whole wing surface. Due to the interference with the cone, the load on the wing results larger than the load on an isolated wing at the same angle of attack.

Direct measurements of the lift and the drag were performed with a three-component sting balance at several angles of attack from −16° to 20°; the results are shown in Figs. 3 and 4. In order to compare the present results with the simple cone configuration, the experimental lift and drag coefficients for a 20° cone[1] are also plotted. In Fig. 3 the lift coefficient and the drag coefficient are plotted against the angle of attack. The values of the lift coefficient computed from the pressure distribution are in good agreement with the balance measurements, so that it appears that the effect of the skin friction and the base drag on the lift is very small compared to the pressure force. Comparing with the isolated cone, it can be seen that a large increase in lift is obtained with the negative dihedral configuration, whereas the positive dihedral gives only a rather small increase. The positive dihedral configuration has a drag coefficient practically equivalent to that of the isolated cone, whereas the negative dihedral has a rather larger drag, especially at large angle of attack. The drag coefficient measured with the balance is larger than that computed from the pressure distribution; the difference (sum of the viscous drag and the base drag) decreases as the angle of attack increases. The viscous drag coefficient has been computed at zero angle of attack, assuming a completely turbulent boundary layer and using the reference enthalpy method; the result is equal to about 0.018; the base pressure coefficient results equal to about 0.04[2]; the sum is equal to 0.058, and it is in good agreement with the experimental results.

A more indicative idea of the difference between the characteristics of the wing-cone configuration and the isolated cone is obtained considering the polar diagram. Figure 4 shows that the polar of the negative dihedral configuration is much flatter than those of the cone and the positive dihedral, especially for large values of C_L. The lift-drag ratio is also plotted in Fig. 4; it appears that the negative dihedral configuration gives a much larger lift-drag ratio than the simple cone and the difference increases with C_L; the positive dihedral configuration gives only a moderate gain with a maximum at about $C_L = 0.5$, whereas for increasing C_L it tends to behave like the cone.

References

[1] Wells, W. R. and Armstrong, W. O., "Tables of Aerodynamic Coefficients obtained from Developed Newtonian Expressions for Complete and Partial Conic and Spheric Bodies at Combined Angles of Attack and Sideslip with some Comparisons with Hypersonic Experimental Data," TR R-127, 1962, NASA.

[2] Zarin, N. A., "Base Pressure Measurements on Sharp and Blunt 9° Cones at Mach Numbers from 3.50 to 9.20," *AIAA Journal*, Vol. 4, No. 4, April 1966, pp. 743–745.

Preionization and Velocity Effects in MHD Channels with Nonequilibrium Plasmas

Lajos L. Lengyel*
Institut für Plasmaphysik, Garching bei München, Germany

RESULTS of numerical computations pertaining to current and potential distributions in MHD channels are reported herein. Unlike in previous studies (see, for example, Refs. 1 and 2) no periodic field distributions have been assumed here. The computations were performed for a Faraday-type channel with a given finite number of electrode pairs. A two-dimensional approximation is used: $\partial/\partial z \equiv 0$, $v \parallel \hat{x}$, and $\mathbf{B} = \text{const} \parallel \hat{z}$. The axial current component was assumed to vanish at upstseam and downstream "infinities." In the mathematical model previously developed for a potassium seeded argon plasma[1,3] allowance is made for nonequilibrium ionization, finite rate recombination,[4] thermal conductivity of the electron gas, and the effect of inelastic collisions on the energy balance of the electrons. A value of 10 was assigned to the inelastic collision loss factor[5] (the magnitude of this coefficient affects primarily the ideal conductivity value and not the relative magnitudes of the preionization and velocity effects). The constant and uniform magnetic field was intentionally kept low enough to avoid nonconvergent (fluctuating) solutions and results whose interpretation may involve speculation. A uniform electron density is prescribed at a certain distance upstream of the first elec-

Received September 9, 1970; revision received November 10, 1970.

* Staff Scientist.